

Upward curvature of the upper critical field and the V-shaped pressure dependence of T_c in the noncentrosymmetric superconductor PbTaSe_2

J. R. Wang¹, Xiaofeng Xu¹ †, N. Zhou¹, L. Li¹, X. Z. Cao¹, J. H. Yang¹, Y. K. Li¹, C. Cao¹, Jianhui Dai¹, J. L. Zhang², Z. X. Shi³, B. Chen⁴, Zhihua Yang⁵

¹Department of Physics and Hangzhou Key Laboratory of Quantum Matters, Hangzhou Normal University, Hangzhou 310036, China

²High Magnetic Field Laboratory, Chinese Academy of Sciences, Hefei 230031, China

³Department of Physics, Southeast University, Nanjing 211189, China

⁴Department of Physics, University of Shanghai for Science & Tehcnology , Shanghai, China

⁵Xinjiang Technical Institute of Physics and Chemistry of Chinese Academy of Sciences, 40-1 South Beijing Road, Urumqi 830011, China

Abstract. The temperature evolution of the upper critical field $H_{c2}(T)$ in the noncentrosymmetric superconductor PbTaSe_2 was determined via resistivity measurements down to 0.5 K. A pronounced positive curvature in the H_{c2} - T phase diagram was observed in the whole temperature range below T_c . The Seebeck coefficient $S(T)$ in the temperature range $5\text{K} \leq T \leq 350\text{K}$ was found to be negative in sign, modest in magnitude and non-linear in temperature. In addition, the superconducting transition temperature T_c under hydrostatic pressure shows a marked non-monotonic variation, decreasing initially with the applied pressure up to $P_c \sim 5$ -10 kbar but then rising with further pressurization. The underlying physical mechanisms of all these findings have been discussed.

PACS numbers: 74.62.Fj, 74.25.fc, 74.25.fg

† Electronic address: xiaofeng.xu@hznu.edu.cn

1. Introduction

Superconductors lacking inversion symmetry have attracted tremendous research interest since the discovery of superconductivity in the noncentrosymmetric (NCS) CePt₃Si [1]. In the presence of inversion symmetry, Cooper pairs are either spin-singlet or spin-triplet, i.e, having well-defined parity. However, in NCS superconductors, the link between spatial symmetry and the Cooper pair spins may be broken and the admixture of singlet-triplet pairing is possible [2, 3, 4]. This is because the antisymmetric spin-orbit coupling (SOC) in the NCS superconductors may split the Fermi surface into two sheets with distinct spin helicities [2, 5]. The splitting of the Fermi surface therefore favors both the intra- and inter-band pairing, resulting in the admixture of spin-singlet and spin-triplet components, with the ratio of these two being tunable by the strength of SOC [2, 6]. Recently, NCS superconductors with *strong* SOC were proposed as potential platforms to realize so-called topological superconductivity [7, 8, 9]. The combination of strong SOC and broken inversion symmetry can give rise to topological superconductivity of class DIII [9].

The NCS compound PbTaSe₂ was recently reported to be superconducting below $T_c \sim 3.7$ K [10]. The crystal structure of PbTaSe₂ consists of stacked hexagonal TaSe₂ layers alternating with Pb monolayers. In the TaSe₂ layer, the Ta atom is located offset from the inversion center. Electronic structure calculations reveal a single Dirac cone in the Brillouin zone which is gapped by ~ 0.8 eV due to large inherent SOC, in analogy to some topologically nontrivial materials [10]. On the other hand, the broken inversion symmetry of the crystal structure along with the large SOC manifests itself as a large band splitting of order of several tenths of an eV. All these features, namely, the lack of inversion symmetry and the strong SOC, appear to fulfill the necessary ingredients for realizing a parity-mixed superconducting state and topological superconductivity. Nevertheless, the superconducting and normal state properties of this material, which may provide valuable clues to the pairing mechanism, and potentially identify possible topological states, have not yet been well characterized.

With this aim in mind, we use electric and thermal transport as a probe to study the superconducting and normal state properties of PbTaSe₂. The upper critical field of PbTaSe₂ was determined by resistivity measurements down to 0.5 K [11, 12], and revealed a prominent upward curvature, regardless of the criteria used to determine H_{c2} . Detailed modelling of the H_{c2} data further suggests two-band superconductivity in PbTaSe₂. The thermoelectric power (TEP) shows the nonlinearity in T and the dominance of negative charge carriers. Remarkably, our pressure study demonstrates a clear V-shaped pressure dependence of T_c , similar to that recently observed in AFe₂As₂ (A=K, Rb, Cs) [13, 14, 15]. The origin of this V-shaped diagram in PbTaSe₂ is possibly due to a Lifshitz transition under pressure, in contrast to the change of pairing symmetry in AFe₂As₂ (A=K, Rb, Cs). Our findings may impose important constraints on any theory of exotic superconductivity in this system and provide some useful indications for the presence or absence of topological states.

2. Experiment

Polycrystalline samples of PbTaSe_2 were prepared by a solid state reaction in evacuated quartz tubes, following similar procedures as given in Ref. [10]. Good crystallinity of the samples was identified by a x-ray powder diffractometer. Traces of an impurity phase of *nonsuperconducting* tantalum oxide, were still detectable. Resistivity was measured by a standard four-probe lock-in technique in a Quantum Design PPMS equipped with a 9 Tesla magnet. For the TEP measurements, a modified steady-state method was used in which a temperature gradient, measured using a constantan-chromel differential thermocouple, was set up across the sample via a chip heater attached to one end of the sample [16, 17, 18]. The thermopower voltage was read out by a nanovoltmeter K2182A from Keithley Instruments. For the hydrostatic pressure measurements, a commercial piston-type cell from Quantum Design was used, and Daphne 7373 oil was applied as the pressure transmission media. For the resistivity curves under pressure, the same contacts were used throughout the measurements such that the geometric errors in the contact size were identical for different pressures.

3. Results And Discussion

Figure 1(a) presents the zero-field resistivity of PbTaSe_2 sample from 350 K down to 2 K. Zero resistivity of the superconducting transition is clearly seen, with the low- T transition expanded in Fig. 1(b). We also note that our transition is slightly broader and the residual resistivity ratio (RRR) is somewhat smaller than that reported in Ref. [10], mostly because of the higher disorder level or slight off-stoichiometry of Se in our samples, considering the high vapor pressure of Se in the reaction. The high- T resistivity rises linearly with temperature above ~ 150 K. This is consistent with its Debye temperature $\Theta_D=143$ K estimated from the heat capacity measurement, indicating the dominance of electron-phonon scattering at this T -range [19]. The superconducting transition at various magnetic fields was studied by the fixed-field temperature sweeps down to ^3He temperatures, presented in Fig. 1(c). In this study, four different criteria have been used to extract the critical temperature at each magnetic field, as exemplified in Fig. 1(b). These criteria include: The onset T_c^{onset} , 90% of the normal state ρ_n $T_c^{90\%}$, middle point $T_c^{50\%}$ and the zero resistance T_c^{zero} .

The resultant H_{c2} - T diagram from these four criteria is cumulatively presented in Fig. 2(a). This diagram features, unlike most of superconductors whose H_{c2} has a negative/downward curvature, the evident upward curvatures for *all* four lines. Note this positive curvature is present for all T below T_c and it becomes very steep for the T_c^{onset} line at low T . This overall upward curvature can not be explained by the Ginzburg-Landau theory, nor by the one-band Werthamer-Helfand-Hohenberg (WHH) model [20]. In Ref. [10], the formula $H_{c2}(T)=H_{c2}(0)(1-t^{3/2})^{3/2}$ was applied to fit the data between 2.4 K to T_c . However, we show in Fig. 2(b) that this formula actually deviates from the experimental data below 1.8 K. Instead, it is possible to

capture the whole data set with the two-band theory, as the upward H_{c2} has also been observed in some two-gap superconductors, e.g., LaFeAsO_{0.89}F_{0.11} [21], MgB₂ [22] and Ca₁₀(Pt₄As₈)((Fe_{1-x}Pt_x)₂As₂)₅ [23]. To analyze our experimental data on a quantitative footing, we now fit the H_{c2} curve with the two-band theory outlined in Ref. [24]. The equation of $H_{c2}(T)$ for a two-band superconductor is given by:

$$\begin{aligned} a_0[lnt + U(h)][lnt + U(\eta h)] + a_1[lnt + U(h)] \\ + a_2[lnt + U(\eta h)] = 0, \end{aligned} \quad (1)$$

where $a_0=2(\lambda_{11}\lambda_{22}-\lambda_{12}\lambda_{21})/\lambda_0$, $a_1=1+(\lambda_{11}-\lambda_{22})/\lambda_0$, $a_2=1-(\lambda_{11}-\lambda_{22})/\lambda_0$, $\lambda_0=\sqrt{(\lambda_{11}-\lambda_{22})^2+4\lambda_{12}\lambda_{21}}$, $h=\frac{H_{c2}D_1}{2\phi_0T}$, $\eta=\frac{D_2}{D_1}$ and $U(x)=\psi(x+\frac{1}{2})-\psi(\frac{1}{2})$. $\psi(x)$ here is the digamma function. λ_{11} , λ_{22} denote the intraband coupling constants, and λ_{12} , λ_{21} are the interband coupling constants. D_1 and D_2 are the diffusivity of each band. The small η may imply a much stronger scattering on one of the bands. Hence, there are totally six free parameters in the fitting process, λ_{11} , λ_{22} , λ_{12} , λ_{21} , D_1 and η . Within this theoretical framework, we fit our experimental data from the 90% of ρ_n criterion, as shown in Fig. 2(b). This two-band theory can overall fit the experimental data within the error bar and the resultant parameters are given in the figure. As can be seen, the intraband coupling slightly dominates the interband coupling while $\eta \ll 1$, indicating that electrons on one band are more scattered than on the other. However, it can *not* be concluded that the two-band superconductivity is wholly responsible for the upward curvature of H_{c2} in this material, in view of the number of free parameters in the fit. In fact, we also fit the data from 50% of ρ_n criterion and obtain $\lambda_{11}=\lambda_{22}=0.5$, $\lambda_{12}=\lambda_{21}=0.4$, $D_1=0.000575$ and $\eta=0.071$, also suggestive of the much stronger scattering on one band. Although these H_{c2} data can not exclusively rule out other possible scenarios, which will be discussed later, they do indicate that two-band superconductivity appears to be a plausible mechanism in PbTaSe₂ [25].

Let us discuss other possible scenarios for the upward curvature in H_{c2} . In the organic superconductor (TMTSF)₂PF₆, H_{c2} also has a pronounced upward curvature and no sign of saturation was observed down to 0.1 K [26]. However, its H_{c2} at $T \rightarrow 0$ K exceeds the Pauli paramagnetic limit by a factor of 2-3. Therefore, the upward curvature was attributed to the signature of spin-triplet pairing. In the case of PbTaSe₂, its H_{c2} at 0.5 K is still much lower than its Pauli limit, suggesting that the orbital effect dominates in limiting its H_{c2} . One theory accounting for the strong upward curvature observed in the cuprates [27, 28] was associated with the quantum critical point in these systems [29]. In our system, however, there is no clear sign to show it is in proximity to the quantum critical regime.

The Seebeck coefficient or TEP reveals important aspects of charge conduction in a material [30, 31]. Figure 3 shows the Seebeck coefficient $S(T)$ of PbTaSe₂ from 350 K down to 5 K. Evidently, its TEP, of modest magnitude, is negative over the entire T -range studied, indicating the dominance of electron carriers. In a single-band metal, according to the Sommerfeld theory, TEP is given by $S=-\frac{\pi^2 k_B^2 T}{2e E_F}$, where E_F

is the Fermi energy [19, 32]. This leads to a T -linear Seebeck coefficient. In reality, the situation may become complicated due to the presence of other excitations. In a metal with both electrons and holes, the electron and hole partial Seebeck coefficients add together according to their weights in conduction [30, 31], i.e., $S = (\frac{\sigma_h}{\sigma})S_h + (\frac{\sigma_e}{\sigma})S_e$. S_h and S_e are the Sommerfeld values (both linear in T) given above. Provided that electron and hole partial weights in conduction also change with T , a nonlinear-in- T Seebeck coefficient can naturally emerge. Indeed, from *ab initio* calculations [10], the Fermi surface of PbTaSe₂ consists of both electron and hole pockets. On the other hand, since the electron pocket dominates, we may apply the single-band Sommerfeld equation quoted above to make a *crude* estimate of the Fermi energy of this material. From Fig. 3, the linear fit at low T gives $E_F \sim 480$ meV.

Shown in Fig. 4(a) is the pressure dependence of the resistivity of PbTaSe₂ up to ~ 25 kbar. With increasing pressure, the resistivity of the sample decreases systematically, while the pressure seems to have little bearing on its overall T dependence. The resistivity at room temperature changes by about 15% at 25 kbar. Interestingly, although the metallicity of the sample is enhanced by the pressure, its T_c shows a nonmonotonic variation, from an initial decrease with pressure to an increase once across a critical pressure, as demonstrated in Fig. 4(b) and 4(c). Note that T_c^{onset} of this sample is about 0.2 K lower than that presented in Fig. 1(b). This discrepancy may arise from the sample off-stoichiometry even if they were harvested from the same batch. Utilizing the same criteria as in Fig. 1(b), we plot the pressure dependence of T_c in Fig. 5(a). Remarkably, regardless of the criteria used, T_c is firstly reduced by the pressure up to $P_c \sim 5-10$ kbar, after which it starts to reverse to higher T_c , similar to the effects of hydrostatic pressure on iron-based superconductors AFe₂As₂ (A=K, Rb, Cs) [13, 14, 15].

The origin of this T_c reversal under pressure has been extensively discussed by F. Tafti *et al.* in their works [13, 14, 15]. This includes a change of the pairing symmetry or a Lifshitz transition across P_c , i.e., an abrupt change of Fermi surface topology. In AFe₂As₂ (A=K, Rb, Cs), they argued that the V-shaped pressure dependence of T_c was the result of a change in pairing symmetry from d -wave state below P_c to an s_{\pm} above P_c . A Lifshitz transition was ruled out in their data, as there were no visible changes in either the Hall or resistivity data across P_c . Following the same procedure given in Ref. [15], we plot the inelastic scattering, defined as $\rho(T=20 \text{ K}) - \rho_0$ where ρ_0 is the residual resistivity at each pressure, as a function of pressure in Fig. 5(b). We should mention that the choice of $T=20$ K is arbitrary but any other cuts above T_c do not affect the results. The plot of $\rho(20\text{K})$ in the inset also shows a similar dependence. In contrast to AFe₂As₂ (A=K, Rb, Cs), the inelastic scattering in PbTaSe₂ displays a sharp drop at a critical pressure somewhere between 5 kbar to 10 kbar (the shaded area in the figure), where T_c also shows a sharp inversion. This makes a compelling case that the T_c reversal in this system is most likely due to a Lifshitz transition around P_c (5-10 kbar).

4. Conclusion

To summarize, we report a strong positive curvature in the H_{c2} - T diagram of the NCS superconductor PbTaSe₂. Its Seebeck coefficient was found to be negative in sign and to vary non-linearly with T . All these experimental data appear to be consistent with a picture of two-band superconductivity in PbTaSe₂, while other possible mechanisms have also been discussed. Interestingly, the recent theoretical proposal of the large Seebeck coefficient arising from topological Dirac fermions has not been seen in our samples [33]. The pressure dependence of the superconducting transition T_c shows a clear 'V' shape, which most likely results from a Lifshitz transition under pressure. Further studies are highly desired to explore the possible parity-mixed state by using ultralow- T thermal conductivity and/or penetration depth measurements.

5. Acknowledgement

The authors would like to thank N. E. Hussey, C. M. J. Andrew, C. Lester, A. F. Bangura, Xin Lu, Zengwei Zhu, Xiaofeng Jin for valuable discussions. This work was supported by the National Key Basic Research Program of China (Grant No. 2014CB648400) and by NSFC (Grant No. 11474080, 11104051, 11104053). X.X. would also like to acknowledge the auspices from the Distinguished Young Scientist Funds of Zhejiang Province (LR14A040001).

References

- [1] Bauer E, Hilscher G, Michor H, Paul C, Scheidt E W, Griбанov A, Seropegin Y, Noel H, Sigrist M and Rogl P 2004 *Phys. Rev. Lett.* **92** 027003
- [2] Yuan H Q, Agterberg D F, Hayashi N, Badica P, Vandervelde D, Togano K, Sigrist M and Salamon M B 2006 *Phys. Rev. Lett.* **97** 017006
- [3] Chen J, Jiao L, Zhang J L, Chen Y, Yang L, Nicklas M, Steglich F and Yuan H Q 2013 *Phys. Rev. B* **88** 144510
- [4] Tafti F F *et al* 2013 *Phys. Rev. B* **87** 184504
- [5] Shimozawa M, Goh S K, Endo R, Kobayashi R, Watashige T, Mizukami Y, Ikeda H, Shishido H, Yanase Y, Terashima T, Shibauchi T and Matsuda Y 2014 *Phys. Rev. Lett.* **112** 156404
- [6] Nishiyama M, Inada Y and Zheng G Q 2007 *Phys. Rev. Lett.* **98** 047002
- [7] Chadov S, Qi X, Kbler J, Fecher G H, Felser C and Zhang S C 2010 *Nat. Mater.* **9** 541
- [8] Lu C K and Yip S K 2010 *Phys. Rev. B* **82** 104501
- [9] Hasan M Z and Kane C L 2010 *Rev. Mod. Phys.* **82** 3045
- [10] Ali M N, Gibson Q D, Klimczuk T and Cava R J 2014 *Phys. Rev. B* **89** 020505
- [11] Niu C Q, Yang J H, Li Y K, Chen B, Zhou N, Chen J, Jiang L L, Chen B, Yang X X, Cao C, Dai J and Xu X 2013 *Phys. Rev. B* **88** 104507
- [12] Zhou N, Xu X, Wang J R, Yang J H, Li Y K, Guo Y, Yang W Z, Niu C Q, Chen B, Cao C and Dai J 2014 *Phys. Rev. B* **90** 094520
- [13] Tafti F F *et al* 2013 *Nat. Phys.* **9** 349
- [14] Tafti F F *et al* 2014 *Phys. Rev. B* **89** 134502
- [15] Tafti F F *et al* 2015 *Phys. Rev. B* **91** 054511
- [16] Xu X, Bangura A F, Niu C Q, Greenblatt M, Yue S, Panagopoulos C and Hussey N E 2012 *Phys. Rev. B* **85** 195101

Upward curvature of the upper critical field and the V-shaped pressure dependence of T_c in the noncentrosym

- [17] Wakeham N, Bangura A F, Xu X, Mercure J F, Greenblatt M and Hussey N E 2011 *Nat. Commun.* **2** 396
- [18] Bangura A F, Xu X, Wakeham N, Peng N, Horii S and Hussey N E 2013 *Sci. Rep.* **3** 3261
- [19] Ashcroft and Mermin, Solid State Physics (Cornell University Press, Cornell, 1975)
- [20] Werthamer N R, Helfand E and Hohenberg P C 1966 *Phys. Rev.* **147** 295
- [21] Hunte F *et al* 2008 *Nature* **453** 903
- [22] de Lima O F, Ribeiro R A, Avila M A, Cardoso C A and Coelho A A 2001 *Phys. Rev. Lett.* **86** 5974
- [23] Mun E, Ni N, Allred J M, Cava R J, Ayala O, McDonald R D, Harrison N and Zapf V S 2012 *Phys. Rev. B* **85** 100502
- [24] A. Gurevich 2003 *Phys. Rev. B* **67** 184515
- [25] In principle, the Hall effect may be used to identify the multiband behaviors. However, the Hall signal in this material is difficult to measure, possibly because of two reasons. First, in the Hall measurements, the sample needs to be thin in order to get large Hall signals, however, our sample is very hard to be cleaved or polished to a thin plate. Second, in a two-carrier model, the Hall coefficient at low fields is given by $R_H = \frac{\sigma_h^2 R_h + \sigma_e^2 R_e}{(\sigma_h + \sigma_e)^2}$, where $\sigma_{e(h)}$ and $R_{e(h)}$ are the conductivity and Hall coefficient of $e(h)$ carriers, respectively (Note that R_e and R_h are opposite in sign). The resultant Hall effect may become very small due to the substantial cancellation of hole and electron components.
- [26] Lee I J, Naughton M J, Danner G M and Chaikin P M 1997 *Phys. Rev. Lett.* **78** 3555
- [27] Mackenzie A P, Julian S R, Lonzarich G G, Carrington A, Hughes S D, Liu R S and Sinclair D C 1993 *Phys. Rev. Lett.* **71** 1238
- [28] Osofsky M S *et al* 1993 *Phys. Rev. Lett.* **71** 2315
- [29] Kotliar G and Varma C M 1996 *Phys. Rev. Lett.* **77** 2296
- [30] Cohn J L, White B D, dos Santos C A M and Neumeier J J 2012 *Phys. Rev. Lett.* **108** 056604
- [31] Cohn J L, Moshfeghyeganeh S, dos Santos C A M and Neumeier J J 2014 *Phys. Rev. Lett.* **112** 186602
- [32] K. Behnia 2009 *J. Phys.: Condens. Matter* **21** 113101
- [33] Xu Y, Gan Z and Zhang S C 2014 *Phys. Rev. Lett.* **112** 226801

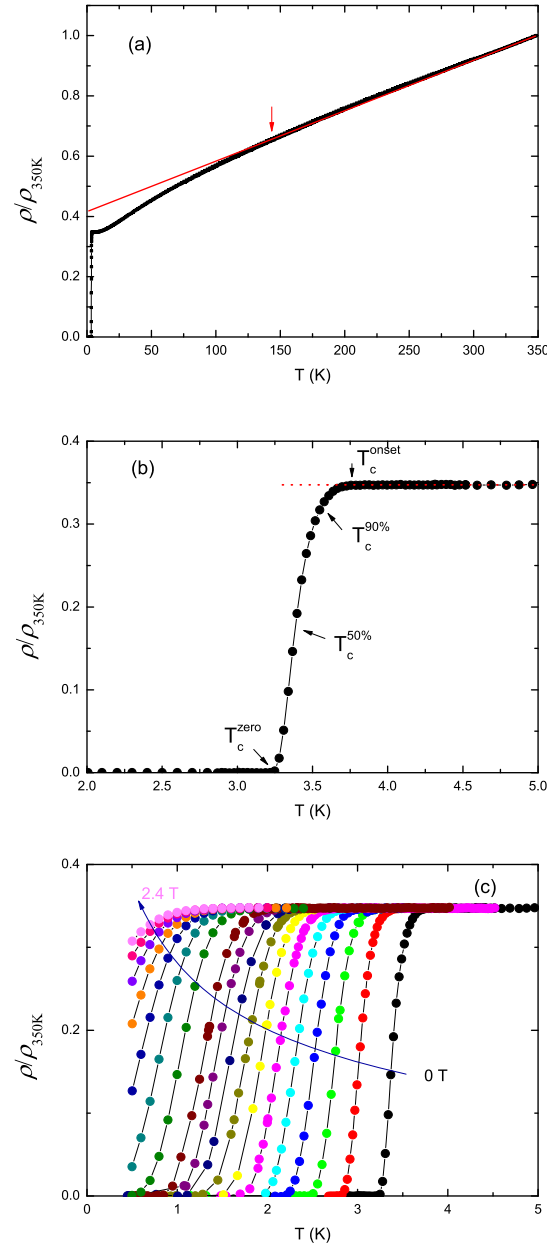


Figure 1. (Color online) (a) Zero-field resistivity of PbTaSe₂ measured from 350 K down to 2 K. The data were renormalized to the 350 K value. Resistivity shows a clear deviation from high- T linearity (red straight line) below ~ 150 K, marked by the arrow. (b) A close-up view of the low- T superconducting transition, illustrating the four criteria used to determine T_c at each field. (c) Superconducting transition under various magnetic fields.

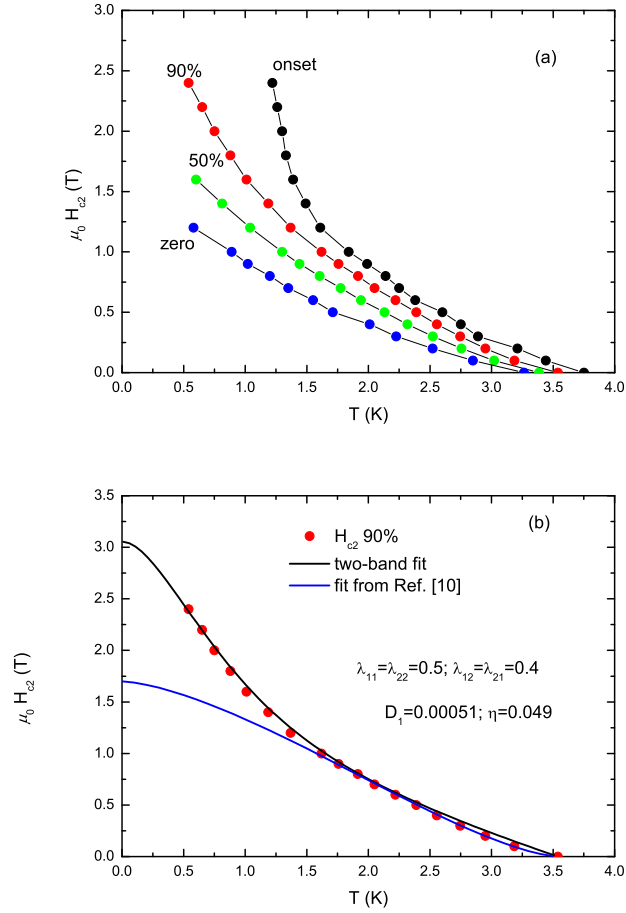


Figure 2. (Color online) (a) Temperature dependence of the upper critical field H_{c2} determined from Fig. 1(c) by using the criteria in Fig. 1(b). (b) The experimental H_{c2} data using the 90% of ρ_n criterion, along with the two-gap fitting described in the text. The blue thin line shows the failure of the fit to the equation $H_{c2}(T)=H_{c2}(0)(1-t^{3/2})^{3/2}$, where t is the reduced temperature T/T_c , used in Ref. [10].

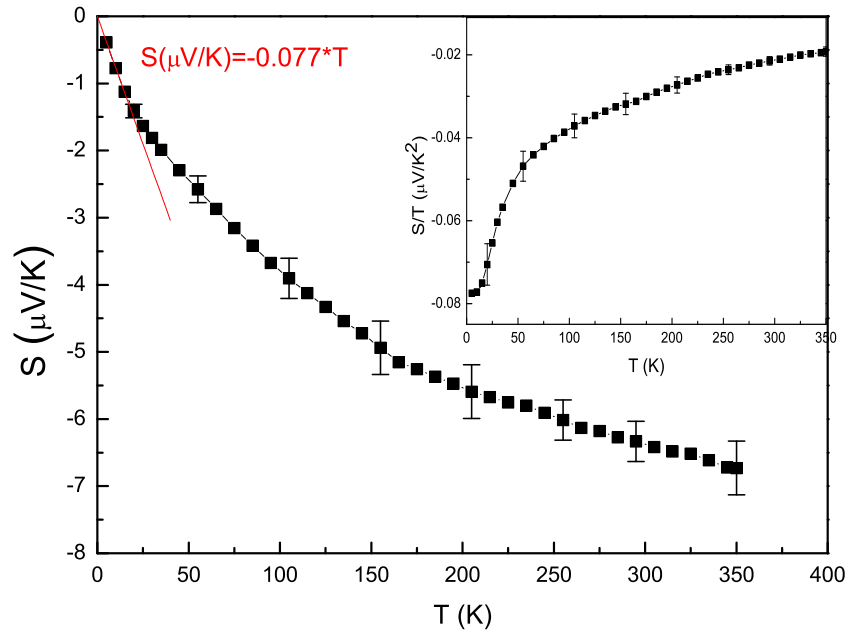


Figure 3. (Color online) The temperature dependence of the Seebeck coefficient measured from 350 K down to 5 K. The typical error bars, estimated from different runs with varying heater currents, were given at certain temperatures. The straight red line is the linear fit to the low- T data. The inset shows the plot of S/T as a function of temperature.

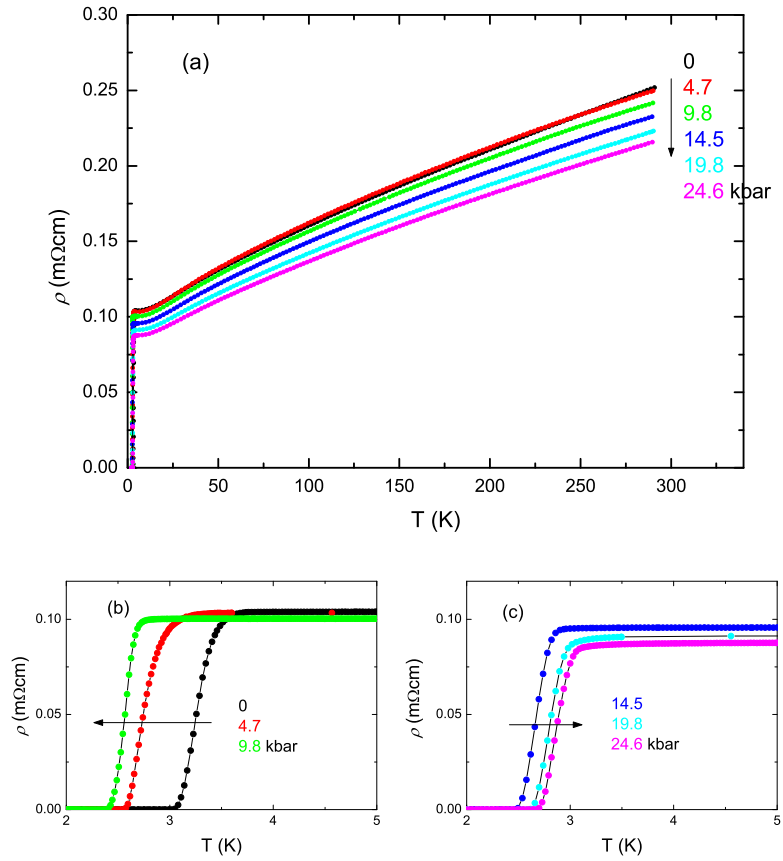


Figure 4. (Color online) (a) shows the resistivity under several pressures, measured by the same electrical contacts. Panels (b) and (c) expand the low- T superconducting transitions under different pressure values.

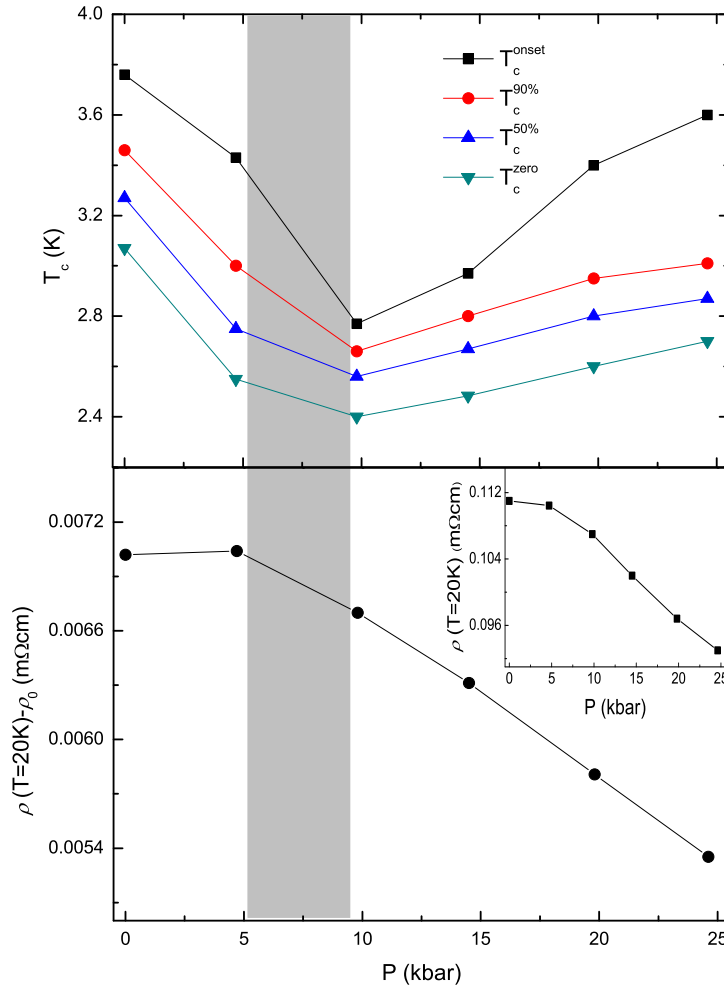


Figure 5. (Color online) (a) shows T_c , estimated by four criteria used in Fig. 1(b), as a function of pressure. (b) The inelastic scattering, defined as $\rho(T=20\text{ K})-\rho_0$ where ρ_0 is the residual resistivity at each pressure, as a function of pressure. The critical pressure where the Lifshitz transition occurs is somewhere in the shaded area. The inset shows $\rho(T=20\text{ K})$ versus pressure.